



Optimization of Joint Blocklength and UAV Placement for UAV-Based Relay Ultra-Reliable Low Latency Communication System

Mohammed J. Mohammed^{*}, Aymen D. Salman[®]

Computer Engineering Department, University of Technology, 10066 Baghdad, Iraq

* Correspondence: Mohammed J. Mohammed (ce.22.05@grad.uotechnology.edu.iq)

Received: 12-21-2024

Revised: 07-01-2025

Accepted: 07-09-2025

Citation: M. J. Mohammed and A. D. Salman, "Optimization of joint blocklength and UAV placement for UAV-based relay ultra-reliable low latency communication system," *Int. J. Comput. Methods Exp. Meas.*, vol. 13, no. 3, pp. 474–483, 2025. <https://doi.org/10.56578/ijcmem130302>.



© 2025 by the author(s). Licensee Acadlore Publishing Services Limited, Hong Kong. This article can be downloaded for free, and reused and quoted with a citation of the original published version, under the CC BY 4.0 license.

Abstract: Drones have a problem with command transmission under Ultra-Reliable Low Latency Communication (URLLC) requirements. This paper discusses minimizing Packet Error Rate (PER) in an Unmanned Aerial Vehicle (UAV) relay system that transmits commands under Ultra-Reliable Low Latency Communication requirements. The problem is solved through joint optimization of block-length allocation and UAV placement. To tackle these challenges, the optimization problem was split into two sub-problems to analyze the convexity and monotonicity of each. An iterative optimization algorithm for PER minimization was then formulated, combining the Alternating Direction Method of the Multipliers algorithm (ADMM) with the bisection search method through a perturbation-based iterative approach. Simulation results confirm that the proposed algorithm achieves up to 16.42% improvement in computation time and up to 57.14% in convergence speed compared to the algorithm using the bisection method alone for both problems, and it gives the same performance as that of the exhaustive search method.

Keywords: Alternating Direction Method of Multipliers; Mission-critical; IoT; URLLC; UAV

1 Introduction

URLLC is a new type of communication that was introduced in Fifth Generation /Beyond Fifth Generation (5G/B5G) to meet the needs of the Internet of Things (IoT), Industry 4.0, and other applications that have strict latency and reliability requirements [1, 2]. Unlike traditional communication systems, URLLC operates under strict constraints, often requiring end-to-end latencies of less than 1 ms and PER as low as 10^{-5} [3, 4]. To guarantee the low-latency transmission of UAV communication systems in URLLC, it uses short packet transmission within a finite packet length [5, 6]. The Shannon formula based on infinite packet length is no longer applicable since PER at the receiver cannot be ignored. To tackle this, Polyanskiy et al. [7] derived the achievable capacity within a finite packet regime to achieve the complex function of the Signal-to-Noise Ratio (SNR), Blocklength, and PER. On the other hand, UAVs have significantly impacted wireless communications due to their advantages, including Line-of-Sight (LoS) aerial-ground connections, rapid deployment, and precise mobility [8, 9]. These features make UAVs suitable for applications requiring reliable and low-latency communication, such as disaster recovery, remote surveillance, and industrial automation. For instance, in scenarios where direct communication between two ground nodes is obstructed by terrain or infrastructure, UAVs can serve as mobile relays, ensuring seamless connectivity [10, 11].

Therefore, one of the effective solutions in the case of communication between two ground points due to obstacles is to use a UAV as a mobile relay [12]. Due to the importance of these benefits, many studies have appeared to benefit from the integration of URLLC and UAV. Minimization of the overall PER by jointly optimizing blocklength allocation and UAV placement in a relay system was studied by Pan et al. [13]. Moreover, the minimization of the overall PER by optimizing blocklength allocation and distance for the Multi-Hop UAV relay system was investigated in the study of Ranjha and Kaddoum [14]. Resource allocation in a two-way UAV relaying system with URLLC was studied by Cai et al. [15]. The optimization of resource allocation and UAV placement in a UAV-based NOMA-based relay system was studied [16]. Although significant progress has been made, several challenges persist, one of the most critical being the urgent need to design and implement fast and efficient algorithms capable of determining the optimal system parameters. Where it is considered that time is a crucial element in such systems, the lack of speed

and precision in identifying these parameters can lead to delays, inefficiencies, or suboptimal performance, which can ultimately compromise the system's effectiveness.

This paper introduces a UAV-based communication system for delivering URLLC services. In the context of military operations, an autonomous robot is assigned the critical role of conducting reconnaissance missions within a designated military zone. It operates remotely, receiving command instructions and relevant information from a central control unit. The aim of the research is to minimize the PER subject to the requirement of reliability and latency by jointly optimizing blocklength allocation for the control unit and the UAV placement. To achieve this, an iterative optimization algorithm was proposed based on the ADMM and the bisection search method for the PER minimization problem.

2 System Model and Problem Formulation

A two-dimensional UAV-based military reconnaissance system was proposed, consisting of a control unit, a UAV, and a robot. The primary function of the UAV is to gather intelligence, assess the environment, and relay vital data back to the command center, as shown in Figure 1. The area between the control unit and the robot has a hill that blocks the line of sight between the sender and the receiver, so the channel gain between them is negligible and weak. That is why using a UAV as a relay as it hovers over the hill to ensure communication and complete the delivery of information.

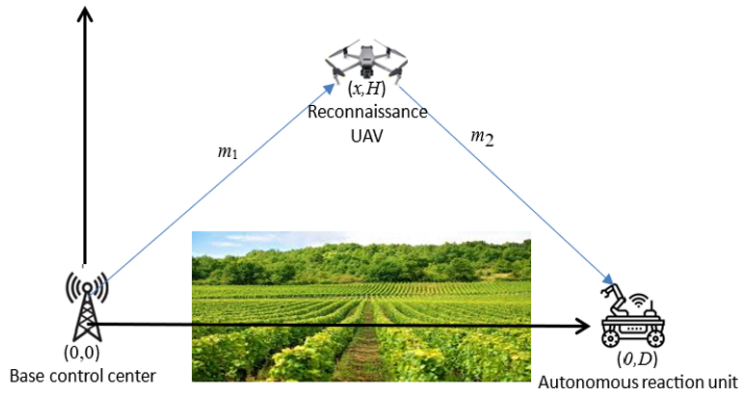


Figure 1. UAV communication system assisted relay for delivering a command under URLLC

The area between the control unit and the robot has a hill that blocks the line of sight between the sender and the receiver, so the channel gain between them is negligible and weak. That is why using a UAV as a relay as it hovers over the hill ensures communication and complete information delivery. The positional coordinates of the control unit, UAV, and autonomous robot are denoted as $(0, 0)$, (x, H) , and $(0, D)$, respectively. These coordinates represent their locations within a Cartesian plane, where the control unit is positioned at the origin with H as the fixed height of the UAV.

Each transmission has two stages: the first stage from the control unit to the UAV and the second stage from the UAV to the robot, or autonomous reaction unit. m_1 and m_2 represent the blocklength allocated for each stage. The system bandwidth is B . Then, the overall blocklength is $M = BT_{\max}$, where T_{\max} is the time in seconds that transmission needs to be complete to transmit a command signal whose packet size is L bits. The channel power gain for the two stages is denoted as h_1 and h_2 , respectively. The transmission powers are fixed from the control unit, P_1 , and the UAV is P_2 , respectively.

The findings in the study of Hashemi et al. [6] indicate that a robust LoS connection is established between the terrestrial control unit and the UAV when it is operating at a specified height, specifically at 120 meters. And can employ the free space channel model in this system. Channel power gain of the link can be mathematically expressed as:

$$h_1 = \frac{\beta_0}{H^2 + x^2}; h_2 = \frac{\beta_0}{H^2 + (D - x)^2} \quad (1)$$

where β_0 is channel power gain at a reference distance, $d_0 = 1$ meter.

As stated by the researches [7, 13, 17], the PER for transition m symbols within a finite packet length of size L is:

$$\varepsilon_i = Q(f(\gamma_i, m_i, L_i)) \quad (2)$$

where, $Q(x)$ is a semantic equation for the above equation ($\varepsilon_i = Q(f(\gamma_i, m_i, L_i))$) and a detailed explanation of the components of the equation.

$Q(x) = \frac{1}{\sqrt{2\pi}} \int_x^\infty e^{-\frac{u^2}{2}} du$ represents the right-tailed function of the standard normal distribution.

$V_i = 1 - \frac{1}{(1+\gamma_i)^2}$, represents channel dispersion.

$\gamma_i = P_i h_i$, represent the Signal-to-Noise Ratio (SNR).

$f(\gamma_i, m_i, L_i) = (\ln 2) \sqrt{\frac{m_i}{V_i}} (\log_2(1 + \gamma_i))$.

Based on this, the PER at the relay is $\varepsilon_1 = Q(f(\gamma_1, m_1, L))$, and the PER for the robot is $\varepsilon_2 = Q(f(\gamma_2, m_2, L))$.

This system assumes that the UAV is a relay that serves as a Decode-and-Forward (DF).

The cumulative PER for the two stages, while ε is defined as follows:

$$\varepsilon = \varepsilon_1 + (1 - \varepsilon_1) \varepsilon_2 \quad (3)$$

The objective of this work is the overall PER minimization due to latency and blocklength restriction to enable URLLC in this system by jointly optimizing blocklength for two stages and the location of the UAV. Consequently, the formulation of the problem optimization is given by Eq. (4) [13, 17]:

$$OP : \min_{\{m_1, m_2, x\}} \varepsilon \quad (4)$$

Provided that m_i must be positive integers $m_{d,m}, m_2 \in z$, with $m_1 + m_2 = M$, and the workable domain for x that primarily relies on the shape of the obstacle $d_1 \leq x \leq d_2$.

The problem in optimization shown in Eq. (4) presents complexity in all its constraints due to the nonconvex nature of the objective function concerning both the location and the blocklength. This complexity persists even when their values are constant, and additionally, the objective function does not exhibit joint convexity concerning the optimization variables.

3 Optimization Algorithm

To solve the problem in Eq. (4), an iterative algorithm was developed to find the optimal UAV placement and blocklength allocation to minimize the effective PER for two stages of the UAV-based relay communication system with finite packet length subject to the latency constraints and reliability requirement. Achieve this by dividing it into two sub-problems. First, find the optimized blocklength with fixed location x . Then, find the optimal location by fixing the blocklength allocation. Finally, alternatively, solve each subproblem until convergence.

3.1 Optimization of Blocklength Allocation With Fixed x

According to the study [1], the channel gains are fixed when the UAV location x is fixed. Therefore, our optimization task focuses solely on the blocklength allocation. It's important to note that the objective function in Eq. (4) is quite complex. Also, to satisfy the reliability requirement, PER should be $\leq 10^{-5}$. The probability of PER at each stage ought to be adequately low. To address this challenge, the overall probability of error ε can be approximately denoted as $\varepsilon(m_1, m_2) \approx \varepsilon_1(m_1) + \varepsilon_2(m_2) \triangleq \tilde{\varepsilon}(m)$. Consequently, to prove that $\tilde{\varepsilon}(m)$ is convex with respect to m_1, m_2 , let $f_1(m_1) = f(\gamma_1, m_1, L)$. The 1st and 2nd-order derivation of $\varepsilon_1(m_1)$ with respect to m could be derived as:

$$\varepsilon'_1 = -\frac{1}{\sqrt{2\pi}} e^{-\frac{f_1^2(m_1)}{2}} f'_1(m_1) \quad (5)$$

$$\varepsilon''_1 = -\frac{1}{\sqrt{2\pi}} e^{-\frac{f_1^2(m_1)}{2}} \left(f_1(m_1) (f'_1(m_1))^2 - f''_1(m_1) \right) \quad (6)$$

Since $e^{-\frac{f_1^2(m_1)}{2}} > 0$ and $f_1(m_1) (f'_1(m_1))^2 > 0$, it is only needed to prove $f''_1(m_1) \leq 0$.

The function f_1 could be simplified by defining $C_1 = \log_2(1 + \gamma_1)$, $A_1 = \frac{\ln 2}{\sqrt{V_1}}$ then, $f_1(m_1)$ and could be written as

$$f_1(m_1) = A_1 \sqrt{m_1} \left(C_1 - \frac{L}{m_1} \right) \quad (7)$$

The 1st and 2nd-order derivation of $f_1(m_1)$ with respect to m_1 is

$$f'_1(m_1) = \frac{1}{2} A_1 C_1 m_1^{-\frac{1}{2}} + \frac{1}{2} A_1 L m_1^{-\frac{3}{2}} \quad (8)$$

$$f''_1(m_1) = -\frac{1}{4} A_1 C_1 m_1^{-\frac{3}{2}} - \frac{3}{4} A_1 L m_1^{-\frac{5}{2}} < 0 \quad (9)$$

Therefore, it explains the exact concavity of the function $f_1(m_1)$ of m_1 . This is proven by the convexity of $\varepsilon_1(m_1)$ with respect to m_1 . The convexity of $\varepsilon_2(m_2)$ with respect to m_2 can be proven by using similar derivations. Thus, the optimal solution to problem 4 can be expressed as:

$$\tilde{\varepsilon}^* = \inf \{ \tilde{\varepsilon} \mid m_1 + m_2 = M \} \quad (10)$$

The proposed ADMM algorithm in the studies [17, 18] was utilized to obtain optimal m_1 and m_2 . Therefore, the Augmented Lagrange Function (ALF) is formulated as

$$L_p = \tilde{\varepsilon} + \lambda(m_1 + m_2 - M) + (\rho/2) \|m_1 + m_2 - M\|_2^2 \quad (11)$$

where, ρ represents the quadratic penalty factor, and λ is the Lagrange multiplier. Eq. (11) combines problem 4 with the constraints by introducing the variable λ . Following a scale transformation, Eq. (11) can be expressed as:

$$L_p = \tilde{\varepsilon} + (\rho/2) \|(m_1 + m_2 - M) + (\lambda/\rho)\|_2^2 \quad (12)$$

Algorithm 1: Find the optimal blocklength allocation (m_1, m_2) with fixed UAV location x

1. **Initialize** $x, \lambda, \rho, M, m_1^{(k)}, m_2^{(k)}$ define maximum iteration is k_{\max} and algorithm accuracy is ϖ .
2. **Repeat**
3. **Update** $m_1^{(k+1)} = \arg \min_{m_1} \tilde{\varepsilon}_1(m_1^{(k)}) + \left(\frac{\rho}{2}\right) \left\| m_1^{(k)} + m_2^{(k)} - M + \frac{\lambda^{(k)}}{\rho} \right\|_2^2$
4. **Update** $m_2^{(k+1)} = \arg \min_{m_2} \tilde{\varepsilon}_2(m_2^{(k)}) + \left(\frac{\rho}{2}\right) \left\| m_1^{(k+1)} + m_2^{(k)} - M + \frac{\lambda^{(k)}}{\rho} \right\|_2^2$
5. **Update** $\lambda^{(k+1)} = \lambda^{(k)} + \rho(m_1^{(k+1)} + m_2^{(k+1)} - M)$
6. **Set** $m_2^{(k+1)} = \text{round}(m_2^{(k+1)}), m_1^{(k+1)} = M - m_2^{(k+1)}$
7. **Until** meeting the convergence condition
8. **Output:** the optimal m_1 and m_2 based on $\tilde{\varepsilon}^*$.

3.2 Optimization of UAV Location With Fixed Blocklength

The objective in this sub-section is to optimize x with a fixed blocklength. Nevertheless, $\tilde{\varepsilon}(x)$ is not convex with respect to x . As in the study [5], we numerically demonstrate the existence of a singular solution that optimally reduces the objective function within the allowable range. Therefore, to be clear, a new function is required to be defined, $g(x) \triangleq \ln \tilde{\varepsilon}(x)$ which is consistent with $\tilde{\varepsilon}(x)$ in monotonicity. Define $f_1(x) = f(\gamma_1, m_1, L), f_2(x) = f(\gamma_2, m_2, L), \gamma_1(x) = \frac{P_1 \beta_0}{H^2 + x^2}$, and $\gamma_2(x) = \frac{P_1 \beta_0}{H^2 + (D-x)^2}$.

The 1st and 2nd order derivative of $g(x)$ with respect to x can be derived as:

$$g'(x) = \frac{\varepsilon'_1(x) + \varepsilon'_2(x)}{\varepsilon_1(x) + \varepsilon_2(x)} \quad (13)$$

$$g''(x) = \frac{(\varepsilon''_1(x) + \varepsilon''_2(x))(\varepsilon_1(x) + \varepsilon_2(x))}{(\varepsilon_1(x) + \varepsilon_2(x))^2} - \frac{\varepsilon'_1(x) + \varepsilon'_2(x)}{(\varepsilon_1(x) + \varepsilon_2(x))^2} \quad (14)$$

where, the 1st and 2nd order derivative of $\varepsilon_1(x)$ is:

$$\varepsilon'_1(x) = \frac{\partial \varepsilon_1(\gamma_1)}{\partial \gamma_1} \gamma'_1(x) \quad (15)$$

$$\varepsilon''_1(x) = \frac{\partial^2 \varepsilon_1(\gamma_1)}{\partial \gamma_1^2} (\gamma'_1(x))^2 + \frac{\partial \varepsilon_1(\gamma_1)}{\partial \gamma_1} \gamma''_1(x) \quad (16)$$

$$\frac{\partial \varepsilon_1(\gamma_1)}{\partial \gamma_1} = -\frac{1}{\sqrt{2\pi}} e^{-\frac{f_1^2(\gamma_1)}{2}} \frac{\partial f_1(\gamma_1)}{\partial \gamma_1} \quad (17)$$

$$\frac{\partial^2 \varepsilon_1(\gamma_1)}{\partial \gamma_1^2} = -\frac{1}{\sqrt{2\pi}} e^{-\frac{f_1^2(\gamma_1)}{2}} \left(f_1(\gamma_1) \left(\frac{\partial f_1(\gamma_1)}{\partial \gamma_1} \right)^2 \right) - \frac{1}{\sqrt{2\pi}} e^{-\frac{f_1^2(\gamma_1)}{2}} \frac{\partial^2 f_1(\gamma_1)}{\partial \gamma_1^2} \quad (18)$$

$$\frac{\partial f_1(\gamma_1)}{\partial \gamma_1} = \sqrt{m} \frac{1 - \ln 2^{\frac{\log_2(1+\gamma_1) - \frac{L}{m_1}}{(1+\gamma_1)^2 - 1}}}{\sqrt{(1+\gamma_1)^2 - 1}} \quad (19)$$

$$\frac{\partial^2 f_1(\gamma_1)}{\partial \gamma_1^2} = Z_1 \left(-\frac{1}{1+\gamma_1} - (1+\gamma_1) \right) \left((1+\gamma_1)^2 - 1 \right) + 3 \ln 2 Z_1 (1+\gamma_1) \left(\log_2 (1+\gamma_1) - \frac{L}{m_1} \right) \quad (20)$$

where, $Z_1 = \frac{\sqrt{m_1}}{\left((1+\gamma_1)^2 - 1 \right)^{\frac{5}{2}}}.$

Thus 1st and 2nd order derivative of $\gamma_1(x)$ is:

$$\gamma'_1(x) = \frac{2P_1\beta_0 x}{(H^2 + x^2)^2} \quad (21)$$

$$\gamma''_1(x) = \frac{6P_1\beta_0 x^4 + 4P_1\beta_0 H^2 x^2 - 2P_1\beta_0 H^4}{(H^2 + x^2)^4} \quad (22)$$

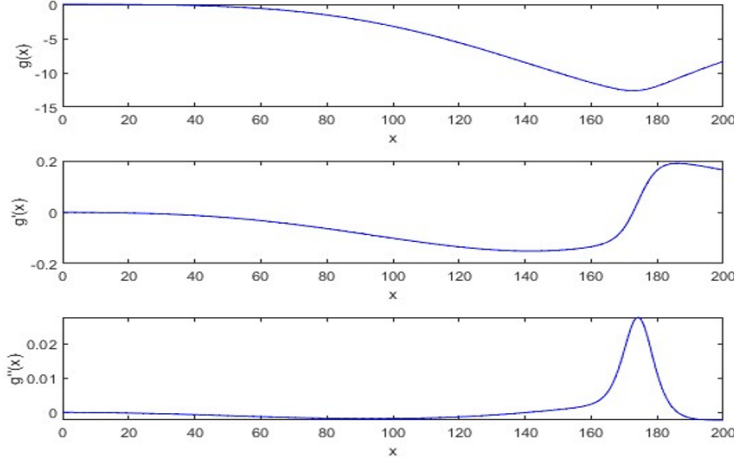


Figure 2. Behavior of $g''(x)$, $g'(x)$ and $g(x)$ functions

Also, 1st and 2nd order derivative $\varepsilon_2(x)$ can be obtained by using the same derivations. After that, it turns out that $g(x)$ is nonconvex with respect to x on all possible intervals of UAV placement. $g(x)$, $g'(x)$, $g''(x)$ plotted in Figure 2 it shows that $g(x)$ is a nonconvex function for the period from $x = 0$ to $x = 142$ because $g''(x)$ is negative. Then, $g(x)$ is a convex function for the period from $x = 142$ to $x = 186$ because $g''(x)$ is positive.

Finally, $g(x)$ is a nonconvex function for the period from $x = 186$ to $x = 200$ because $g''(x)$ is negative. Nonetheless, observations indicate that for the period from $x = 0$ to $x = 173$, the $g'(x)$ is negative and for the period from $x = 173$ to $x = 200$ the $g'(x)$ is positive. This means the value of it reduces until $x = 173$, then rises. From this, it was noted that $g(x)$ is quasiconvex, and there is a distinct x that can optimize the overall effective PER, and Algorithm 2 can be applied to this task.

Algorithm 2: Find the optimal UAV' location (x) with fixed blocklength (m_1, m_2)

1. **Initialize** error tolerance $\zeta = 0.1$, $x^{lb} = d_l$ and $x^{ub} = d_2$
2. **if** $g'(x)|_{x=d_1} > 0$ **then**
3. **return** $x^* = d_1$
4. **else**
 - continue*
5. **If** $g'(x)|_{x=d_2} < 0$ **then**
6. **return** $x^* = d_2$
7. **else**
 - Repeat**
 - 9. $x^{\text{mid}} = (x^{ub} + x^{lb}) / 2.$
 - 10. **If** $g'(x)|_{x=x^{\text{mid}}} > 0$ **then**
 - 11. $x^{ub} = x^{\text{mid}}$
 - 12. **Else**
 - 13. $x^{lb} = x^{\text{mid}}$
 - 14. **End**
 - 15. **Until** $x^{ub} - x^{lb} > \zeta$ **Do**
 - 16. **End**
 - 17. **End**

3.3 Overall Algorithm and Analysis

Algorithm 3 combines the previous two algorithms within an iterative framework, utilizing a random integer R_{\max} . It initializes the variables and then determines the optimal blocklengths m_1 and m_2 for the default location by using Algorithm 1. Subsequently, it adds a random number to the blocklengths obtained from Algorithm 1 and identifies three locations for the UAV using Algorithm 2. It then selects the location with the least PER and its corresponding blocklength, repeating the process. This ensures that the algorithm converges to a solution as long as the PER decreases with each iteration.

Algorithm 3: Overall iterative optimization algorithm for optimizing m_1 , m_2 , and	
1.	Initialize $k_{\max}, k = 1, R_{\max}, x^{(k)}, m_1^{(k)}, m_2^{(k)}$
2.	while $k \leq k_{\max}$ do
3.	Use algorithm 1 to obtain $m_1^{(k)}, m_2^{(k)}$ by $x_m^{(k)}$
4.	Generate 2 integers randomly r^a, r^b in the period $[1, R_{\max}]$
5.	Use Algorithm 2 to obtain x_a by using $m_1 = m_1^{(t)} - r^a$ and $m_2 = m_2^{(t)} + r^a$
6.	Use Algorithm 2 to obtain x_b by using $m_1 = m_1^{(t)} + r^b$ and $m_2 = m_2^{(t)} - r^b$
7.	From x_m, x_a, x_b Select the x who achieves a minimum $\tilde{\varepsilon}(m)$ and label it as $x^{(k)}$
8.	Set $k = k + 1$;
9.	End

The complexity of the ADMM algorithm depends on the specific problem structure and the criteria for convergence that are employed. For each iteration, the complexity is linear concerning the number of variables when the algorithm is applied to separable problems. Nonetheless, the aggregate complexity is variable based on specific problem structures and the convergence criteria implemented.

In specific scenarios, particularly in instances where the resolution of the problem necessitates matrix inversions or factorizations within the optimization procedure, the complexity can escalate to a cubic relationship, denoted as N^3 [7, 19, 20]. Therefore, the complexity of Algorithm 1 is given by $Q_1 = O(N^3)$, and for Algorithm 2 is given by $Q_2 = O(\log_2((d_2 - d_1)/\zeta))$. Since Algorithm 3 calls Algorithm 2 three times every time it calls Algorithm 1 in every iteration, the complexity of Algorithm 3 is $Q_3 = O(n_{\max}(Q_1 + Q_2))$.

Although the complexity of this algorithm is theoretically higher than the algorithm based on a bisection search method, it has shown fast convergence. On the other hand, the complexity of this problem is low due to its separable nature, and there are no matrix operations. And the appropriate selection of ρ has been instrumental in accelerating the convergence.

Table 1. System parameters

Parameter	Value
Robot distance (D)	200 meter
Number of bits (L)	100 bits
The start point of the obstacle (d_1)	30 meter
The endpoint of the obstacle (d_2)	130 meter
Initial UAV location (x)	30 meter
Transmit power of CU (P_1)	3 Watt
Transmit power of UAV (P_2)	1 Watt
Time for transmit command signal (T_{\max})	10^{-4} sec
Bandwidth (B)	1 MHz
Number of available blocklength ($M = BT_{\max}$)	100
Initial blocklength for each stage $m_1 = m_2 = \frac{M}{2}$	50
Channel power gain at a reference distance (β)	50 db
Location accuracy (ξ)	0.1 meter
Random integer range (R_{\max})	3
Regularization parameter for ADMM (λ)	0
Penalty factor (ρ)	0.007
ADMM algorithm accuracy (ϖ)	10^{-6}
Max Number of iterations (k_{\max})	10

3.4 System and Algorithm Parameters

The parameter values for the system model used in this paper are listed in Table 1. It is worth noting that most parameters were used from [13, 17], and some variables were adjusted based on the results obtained during the

simulation, as they were found to be the most suitable. It's important to highlight that all our simulations were carried out using MATLAB® R2023a on a PC with an Intel i7-1165G7 processor and 8G RAM.

4 Results and Discussion

The convergence behavior of Algorithm 3 is plotted in Figure 3 for different values of the penalty factor for ADMM and fixed UAV altitude. It shows the penalty factor has a high effect on the convergence in terms of overall PER and the number of iterations needed to reach the stable value. So, whenever the value is greater or less than 0.007, it makes the behavior of the algorithm unstable, and the best value is 0.007 to ensure the stability of the algorithm's convergence. Approximated decoding error probability

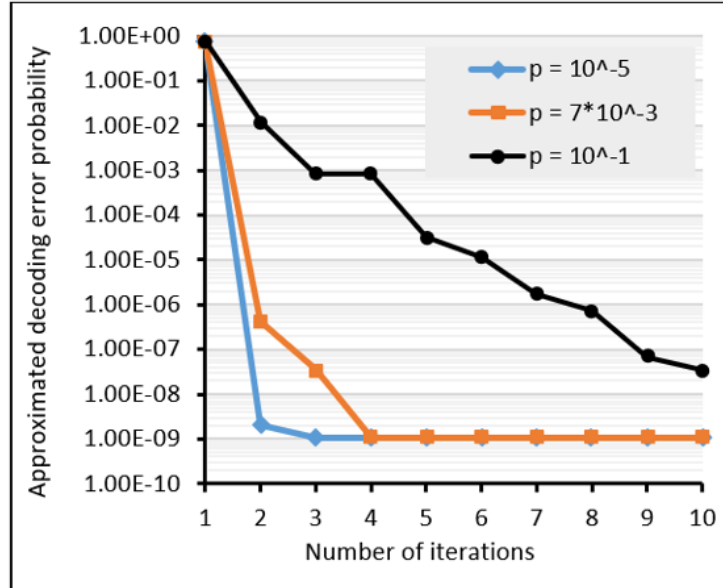


Figure 3. Convergence behavior of Algorithm 3 for fixed H and different penalty factor (ρ) values

The convergence of Algorithm 3 is plotted in Figure 4 and compared to the exhaustive search method. The results show that the proposed algorithm achieved the same performance as the exhaustive search method despite the nonconvex nature of the problem. This demonstrates the effectiveness of the proposed algorithm in avoiding costly computations while maintaining accuracy. However, optimal performance depends on the choice of initial parameters, such as ρ , as inappropriate values may lead to unstable convergence. Therefore, further studies are recommended to explore mechanisms for dynamically adapting these parameters to improve performance under variable channel conditions.

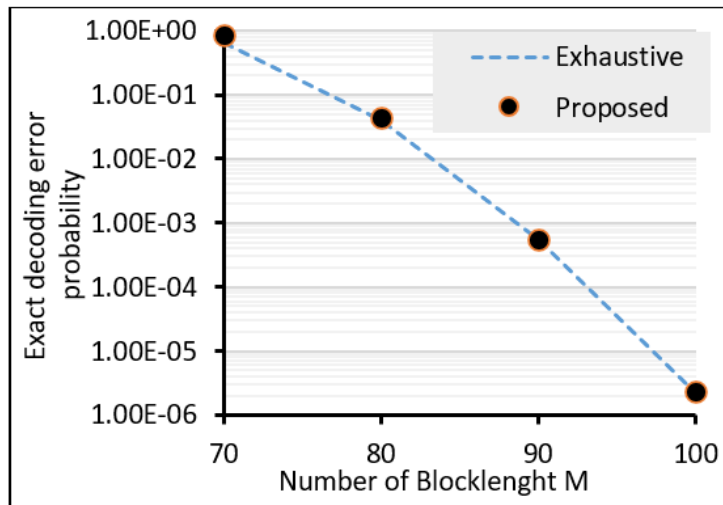


Figure 4. Comparison of the proposed algorithm with the exhaustive search algorithm

Figure 5 compares Algorithm 3 to the algorithm in the study [13] that used the bisection search method to optimize the block length. The comparison demonstrates an improvement of up to 57.14% in convergence speed to the optimum value compared to the bisection method-based algorithm. This improvement is attributed to the ADMM algorithm's efficiency and ability to achieve rapid convergence by optimizing partial factors such as the penalty factor, ρ . Furthermore, using the bisection method to determine the UAV's position effectively reduced PER, reflecting the algorithm's ability to balance reliability and efficiency.

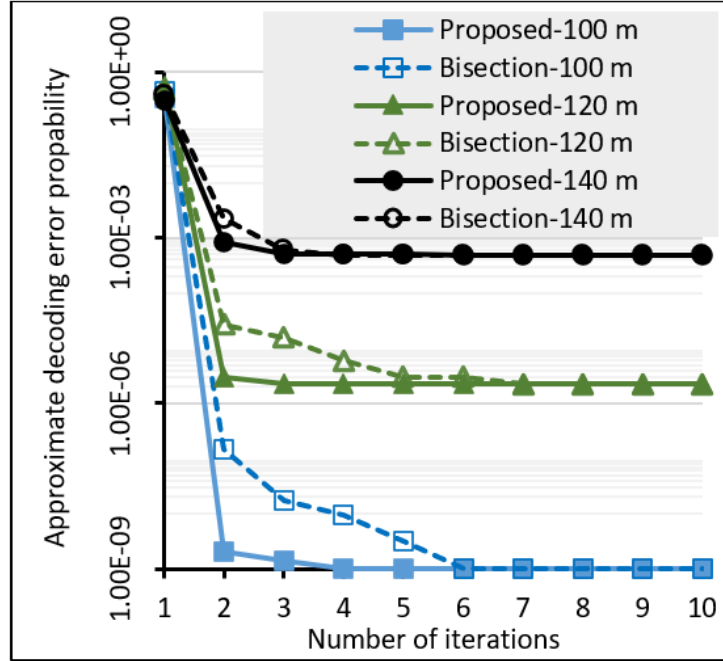


Figure 5. The proposed algorithm convergence behavior with comparison to the algorithm based on the bisection search method

Furthermore, the computation time for the algorithms was calculated and presented in Table 2, showing a notable optimization in execution time with an acceleration of approximately 16.42% across ten iterations. This optimization becomes even more significant when considering that the proposed algorithm converges to the optimal value faster than the bisection-based method.

Table 2. Computation time for the proposed algorithm and other algorithms

Algorithm	Computation Time (second)
Proposed Algorithm	2.773
Bisection method-based	3.318
Exhaustive search method	59,337.78

5 Conclusions

This paper introduced the blocklength allocation and UAV placement optimization in a UAV-based relay system that achieves the requirement of URLLC in terms of reliability and latency. Firstly, the problem of reducing the overall PER was split into two subproblems. Then, the ADMM algorithm is applied to solve blocklength allocation, and the bisection search method is used to solve UAV placement optimization. Finally, these two problems were combined by an iterative algorithm to reach the values of the optimal UAV placement and blocklength allocation that minimize PER.

The proposed algorithm requires careful tuning of the penalty factor to achieve optimal results. The choice of it depends on the selected scenario, as different channel conditions and system configurations may require adjustments for stability and efficiency. When selecting the appropriate value of the penalty factor, the algorithm demonstrated significant improvements in convergence speed, reducing the PER by up to 57.14% compared to the bisection search method. Additionally, the computation time was reduced by 16.42%, enhancing its efficiency for real-time communication applications and latency-sensitive systems.

Based on these findings, we recommend implementing adaptive blocklength allocation mechanisms that can respond to changing channel conditions in real-time and deploy multiple UAVs in areas with high user density to distribute the communication load better. The promising computational efficiency demonstrated by the proposed algorithm offers a foundation for real-time implementations, paving the way for its integration into advanced adaptive communication protocols.

Data Availability

The data used to support the findings of this study are available from the corresponding author upon request.

Conflicts of Interest

The authors declare that they have no conflicts of interest.

References

- [1] T. K. Le, U. Salim, and F. Kaltenberger, “An overview of physical layer design for ultra-reliable low-latency communications in 3GPP releases 15, 16, and 17,” *IEEE Access*, vol. 9, pp. 433–444, 2020. <https://doi.org/10.1109/access.2020.3046773>
- [2] H. D. Albonda, “Radio control optimization for enhanced QoS-based spectrum selection in heterogeneous 5G environments with eMBB and uRLLC,” *Int. J. Intell. Eng. Syst.*, vol. 16, no. 6, pp. 542–552, 2023. <https://doi.org/10.22266/ijies2023.1231.45>
- [3] M. N. Abdullah and M. A. Alsaedi, “A survey-resources management in 5G mobile networks,” *Al-Iraqia J. Sci. Eng. Res.*, vol. 1, no. 1, pp. 21–43, 2022. <https://doi.org/10.33193/ijser.1.1.2022.35>
- [4] C. M. W. Basnayaka, D. N. K. Jayakody, and Z. Chang, “Age-of-information-based URLLC-enabled UAV wireless communications system,” *IEEE Internet Things J.*, vol. 9, no. 12, pp. 10 212–10 223, 2021. <https://doi.org/10.1109/JIOT.2021.3123431>
- [5] C. Feng, H. M. Wang, and H. V. Poor, “Reliable and secure short-packet communications,” *IEEE Trans. Wirel. Commun.*, vol. 21, no. 3, pp. 1913–1926, 2021. <https://doi.org/10.1109/TWC.2021.3108042>
- [6] R. Hashemi, S. Ali, N. H. Mahmood, and M. Latva-aho, “Average rate and error probability analysis in short packet communications over RIS-aided URLLC systems,” *IEEE Trans. Veh. Technol.*, vol. 70, no. 10, pp. 10 320–10 334, 2021. <https://doi.org/10.1109/TVT.2021.3105878>
- [7] Y. Polyanskiy, H. V. Poor, and S. Verdú, “Channel coding rate in the finite blocklength regime,” *IEEE Trans. Inform. Theory*, vol. 56, no. 5, pp. 2307–2359, 2010. <https://doi.org/10.1109/TIT.2010.2043769>
- [8] X. Guo, B. Li, D. Zhai, and R. Zhang, “Performance analysis and optimization of a UAV-enabled two-way relaying network under FSMH, NC, and PNC schemes,” *IEEE Internet Things J.*, vol. 8, no. 24, pp. 17 802–17 816, 2021. <https://doi.org/10.1109/JIOT.2021.3083648>
- [9] A. A. Kareem, M. J. Mohamed, and B. K. Olewi, “Unmanned aerial vehicle path planning in a 3D environment using a hybrid algorithm,” *Bull. Electr. Eng. Informatics*, vol. 13, no. 2, pp. 905–915, 2024. <https://doi.org/10.11591/eei.v13i2.6020>
- [10] A. A. Kareem, B. K. Olewi, and M. J. Mohamed, “Planning the optimal 3D quadcopter trajectory using a delivery system-based hybrid algorithm,” *Int. J. Intell. Eng. Syst.*, vol. 16, no. 2, pp. 427–439, 2023. <https://doi.org/10.22266/ijies2023.0430.34>
- [11] H. Qays, A. Salman, and B. Jumaa, “Autonomous quadcopter delivery system,” *J. Xi'an Univ. Archit. Technol.*, vol. 12, no. 4, pp. 1504–1516, 2020. <https://doi.org/10.37896/jxat12.04/886>
- [12] D. H. Tran, V. D. Nguyen, S. Chatzinotas, T. X. Vu, and B. Ottersten, “UAV relay-assisted emergency communications in IoT networks: Resource allocation and trajectory optimization,” *IEEE Trans. Wirel. Commun.*, vol. 21, no. 3, pp. 1621–1637, 2021. <https://doi.org/10.1109/TWC.2021.3105821>
- [13] C. Pan, H. Ren, Y. Deng, M. Elkashlan, and A. Nallanathan, “Joint blocklength and location optimization for URLLC-enabled UAV relay systems,” *IEEE Commun. Lett.*, vol. 23, no. 3, pp. 498–501, 2019. <https://doi.org/10.1109/LCOMM.2019.2894696>
- [14] A. Ranjha and G. Kaddoum, “Quasi-optimization of distance and blocklength in URLLC-aided multi-hop UAV relay links,” *IEEE Wirel. Commun. Lett.*, vol. 9, no. 3, pp. 306–310, 2019. <https://doi.org/10.1109/LWC.2019.2953165>
- [15] Y. Cai, X. Jiang, M. Liu, N. Zhao, Y. Chen, and X. Wang, “Resource allocation for URLLC-oriented two-way UAV relaying,” *IEEE Trans. Veh. Technol.*, vol. 71, no. 3, pp. 3344–3349, 2022. <https://doi.org/10.1109/TVT.2022.3143174>
- [16] J. Ji, K. Zhu, D. Niyato, and R. Wang, “Joint cache placement, flight trajectory, and transmission power optimization for multi-UAV assisted wireless networks,” *IEEE Trans. Wirel. Commun.*, vol. 19, no. 8, pp. 5389–5403, 2020. <https://doi.org/10.1109/TWC.2020.2992926>

- [17] H. Hu, H. Han, Y. Huang, Q. Kang, J. Si, S. Zhao, and J. Wang, “Reliability analysis for NOMA-based UAV assisted short packet communication,” *IET Commun.*, vol. 17, no. 16, pp. 1917–1927, 2023. <https://doi.org/10.1049/cmu2.12661>
- [18] S. Boyd, N. Parikh, E. Chu, B. Peleato, and J. Eckstein, “Distributed optimization and statistical learning via the alternating direction method of multipliers,” *Found. Trends® Mach. Learn.*, vol. 3, no. 1, pp. 1–122, 2011. <https://dx.doi.org/10.1561/2200000016>
- [19] T. Y. Lin, S. Q. Ma, and S. Z. Zhang, “On the sublinear convergence rate of multi-block ADMM,” *J. Oper. Res. Soc. China*, vol. 3, pp. 251–274, 2015. <https://doi.org/10.1007/s40305-015-0092-0>
- [20] J. Wang, F. Yu, X. Chen, and L. Zhao, “ADMM for efficient deep learning with global convergence,” in *Proceedings of the 25th ACM SIGKDD International Conference on Knowledge Discovery & Data Mining*, 2019, pp. 111–119. <https://doi.org/10.1145/3292500.3330936>

Nomenclature

B	System bandwidth, Hz
x	UAV’s horizontal coordinate, meter
H	UAV’s fixed altitude, meter
D	Distance between the control unit and the robot, meters
L	Packet size, bits
M	Overall blocklength, Symbol
T_{\max}	Maximum latency constraint, meter
P_1, P_2	Transmission power of the control unit and UAV, watts

Greek symbols

β	Channel power gain at a reference distance
γ	Signal-to-Noise Ratio (SNR)
ε	Packet Error Rate (PER)
λ	Lagrange multiplier
ρ	Quadratic penalty factor

Subscripts

i	Index for transmission stages ($i = 1, 2, \dots$)
max	Maximum value
mid	Midpoint value
lb, ub	Lower bound and upper bound